AGRICULTURE AND NATURAL RESOURCES

Journal homepage: http://anres.kasetsart.org

Research article

Influence of monsoon-forced Ekman transport on sea surface height in the Gulf of Thailand

Minobu Higuchi[a,†], Monton Anongponyoskun[b,†], Jitraporn Phaksopa[b,†], Hiroji Onishi[c,*]

[a] *School of Fisheries Sciences, Hokkaido University, Hakodate, Hokkaido 041-8611, Japan.*

[b] *Department of Marine Science, Faculty of Fisheries, Kasetsart University, Bangkok 10900, Thailand.*

[c] *Faculty of Fisheries Sciences, Hokkaido University, Hakodate, Hokkaido 041-8611, Japan.*

Article Info

Article history:
Received 30 May 2019
Revised 2 November 2019
Accepted 2 March 2020
Available online 31 March 2020

Keywords:
Ekman transport,
Gulf of Thailand,
Indian Ocean Dipole

Abstract

The influence of monsoon-forced Ekman transport on sea surface height in the Gulf of Thailand (GoT) was analyzed using globally standardized air-sea physical data from multiple satellite and in situ observations extracted from COPERNICUS, the Marine Environment Monitoring Service of the European Commission. Monthly datasets from the period 2010–2016 showed that sea surface height variation in the GoT (as an objective variable: Y) was strongly correlated (correlation coefficient = 0.955, $p < 0.01$, n = 83) with Ekman transport across the GoT mouth, based on the estimation of wind stress in the area open to the South China Sea (SCS). One explanatory variable was variation in Ekman transport (X_1) and another was variation in the averaged dynamic height in the GoT (X_2). The standard regression coefficient indicated that the influence of Ekman transport by surface wind was approximately seven times larger than that of dynamic height by GoT hydrographic conditions. Monsoonal wind systems were dominant in the sea surface of both the GoT and SCS. In summer, the dominant southwesterly wind generated outflow transport of surface water from the GoT toward the SCS, which promoted estuarine circulation at the GoT mouth. In winter, the dominant northeasterly wind promoted inverse estuarine circulation. During the strong positive Indian Ocean Dipole, the southwesterly monsoonal wind increased and circulation in the GoT was enhanced.

Introduction

The Gulf of Thailand (GoT) is a wide, shallow basin on the continental shelf of Southeast Asia. Its average depth is approximately 58 m (maximum, 85 m) and it covers an area of about 270,000 km^2 (length, 800 km; width, 560 km). The GoT is largely enclosed by the landmass of Thailand, Cambodia, and Malaysia and is linked to the South China Sea (SCS). In general, the GoT and SCS are divided by an imaginary line connecting Cape Ca Mau (Indochina Peninsula) and Kota Bharu (Malaysia Peninsula). The GoT provides important littoral services, such as fishing grounds, shipping routes, and recreational areas, but it is also subject to illegal waste dumping and dwindling living resources and deteriorating water quality in the GoT are of serious concern (Cheevaporn and Menasveta, 2003; Pauly and Chuenpagdee, 2003; Qiao et al., 2015).

Water circulation in the GoT and water exchange with the SCS through the GoT mouth are important to marine environmental conditions. However, the circulation pattern of water flow and water exchange ratio in the GoT has been poorly studied. Yanagi et al. (2001) indicated that the density-driven current is induced by the

† Equal contribution.
* Corresponding author.
E-mail address: onishi@fish.hokudai.ac.jp (H. Onishi)

https://doi.org/10.34044/j.anres.2020.54.2.12

horizontal density difference between the warm surface water in the GoT and cold SCS water in the inter-monsoon season (April–May). These authors further mentioned that even in the maximum river discharge season after the dominant southwesterly monsoon, the water exchange ratio is weaker than that in the inter-monsoon season. Buranapratheprat et al. (2016) used local model results to show that water intrusion in the deep layers of the SCS starts in April and ends in November, which is expected to occur when the surface temperature of the GoT is warmer than that of the SCS in summer. Therefore, the density-driven circulation generates surface outward flow, encouraging Ekman transport through southwesterly monsoon winds. On the other hand, Buranapratheprat et al. (2016) deduced that Ekman transport by northeasterly monsoon winds maintains the low salinity of GoT surface water.

Using long-term sea-level data from tide gauges, Yanagi and Akaki (1994) and Vongvisessomjai (2006) indicated that the mean sea level of the GoT showed few depressions in decadal historical data, which might have been due to plate tectonics. However, they predicted that changes in sea level would be complicated by the larger effects of glacioeustasy and ocean-atmospheric activities. In light of natural disasters in coastal areas, such as storm surges, tsunamis and flooding, the sea surface height (SSH) in the GoT must be studied.

Both tide gauge and satellite altimetry data show clear annual cycles (minimum in summer and maximum in winter, with differences exceeding 0.4 m) in the GoT (Sojisuporn et al., 2010; Trisirisatayawong et al., 2011). Such annual cycles do not consist of annual variations in dynamic height in the GoT. The purpose of the present study was to estimate the effect of Ekman transport and hydrographic conditions on the annual SSH cycle of the GoT.

Materials and Methods

All data were taken from the COPERNICUS Marine Environment Monitoring Service datasets (a European Program for the establishment of a European capacity for Earth Observation): MULTIOBS_GLO_PHY_REP_015_002, and WIND_GLO_WIND_L4_ REP_OBSERVATIONS_012_003. Monthly mean SSH, sea surface temperature (SST) and sea surface salinity (SSS) data were obtained from the former dataset on a 0.25° × 0.25° longitude-latitude grid for 2010–2016, and monthly mean wind field data for the same period were obtained from the latter dataset based on the same grid resolution.

The details of both datasets are described in the COPERNICUS product data sheet (Driesenaar et al., 2016; Bentamy, 2017; Verbrugge, 2018a; Verbrugge, 2018b). Monthly mean SSH and SST data were obtained from satellite observation and reprocessed using a multiple linear regression and covariances deduced from historical observations, which produced synthetic fields. The synthetic fields and all available in situ T/S profiles were combined using an optimal interpolation method. The vertical field of the dataset consisted of 33 layers to a depth of 5,500 m, of which five layers (0 m, 10 m, 20 m, 30 m and 50 m) were used in this study, in light of the average depth of the GoT. The wind field data were obtained from ASCAT scatterometers onboard METOP-A satellites and included monthly averaged wind speed and stress data. These consisted of zonal and meridional wind components. The monthly winds were estimated at each grid point (0.25° × 0.25°) from at least 25 daily values available at the same grid point. Moreover, the wind stress data were calculated using an air concentration constant (1.225 kg/m^3) and drag coefficient (C_D), with linear responses to wind speed set to the upper limit. However, the February 2010 wind data were not used in the current study because they were absent from the dataset.

The study area comprised the GoT and southwestern part of the SCS (Fig. 1). Fig. 1 shows the space-averaged area for temperature, salinity, dynamic height and SSH in area A and the wind field in area A' within the GoT. as well as the wind field in area B in the GoT mouth, set not to overlap with area A'. The GoT mouth line was set to stretch between Kota Bharu in Malaysia and Cape Cà Mau in Vietnam (azimuth, 45°T; length, 390.6 km).

Ekman volume transport (E.T.) in the GoT mouth was estimated using Equation 1 from Pedlosky (1987):

$$\text{E.T.} = \frac{\tau}{\rho f} \times L \times 10^{-6} \quad (1)$$

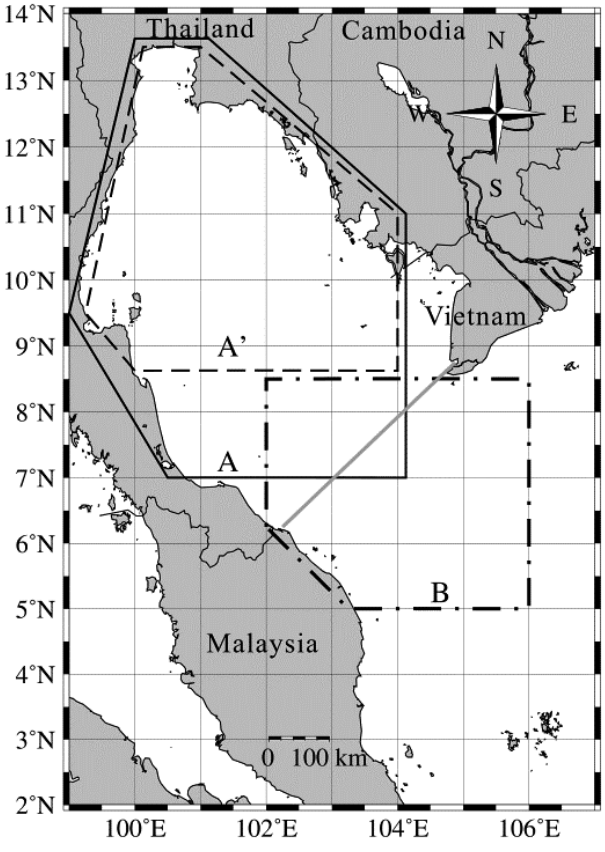

Fig. 1 Study area in the Gulf of Thailand (GoT) and southwestern part of the South China Sea. Area A shows the average area for temperature, salinity, dynamic height and sea surface height; areas A' and B show the average area for wind field within the GoT and at the mouth of the GoT, respectively, and were set not to overlap

where τ is wind stress along the azimuth 45°T spatially averaged in the GoT mouth (area B), ρ is the sea surface density calculated using T/S data and spatially averaged in the mouth area, f is the Coriolis parameter based on latitude 7°N ($1.78 \times 10^{-5} s^{-1}$), and L is width of the GoT mouth (390.6×10^3 m). To express the values of Ekman volume transport in the unit Sv, it was multiplied by 1×10^{-6}.

Results and Discussion

Annual variations

Annual variations in hydrographic conditions averaged over 7 yrs in the GoT are shown in Fig. 2. SST peaked in May, the inter-monsoon season, and SSS had a definite minimum in October, the end of the rainy season (southwesterly monsoon). The dynamic height, which was calculated by integral dynamic depth anomalies at each standard depth from the 50 m reference level to the surface (0–50 m/50 m), had two peaks in May and October. The most prominent peak depended on the SST and upper-layer maximum temperature in the GoT, whereas the second depended on the SSS and upper-layer lowest salinity. Fig. 3 shows the annual cycle of the SSH and sea surface wind of the southwest components in the GoT (area A') and GoT mouth (area B). Variations in SSH had two phases, namely the lowest phase in summer (June–September) and the highest phase in winter (December–January); other months connected these two phases almost linearly.

The southwest wind components in areas A' and B had incoherent phases in terms of SSH variation. Southwest and northeast components were strong in summer and winter, respectively. In area A', the southwest components were higher than those in area B. In contrast, the northeast components were higher in area B than in area A' because of the protection granted by the Indochina peninsula during the northeasterly monsoon to the inside of the GoT and by the mountains in central Malaysia during the southwesterly monsoon to the mouth of the GoT. The standard deviation for all variables (SST, SSS and dynamic height in Fig. 2, and SSH and southwest-northeast wind components in Fig. 3) over the study period were not expressed, as they were compared to their seasonal variation. Standard deviations were slightly larger during the inter-monsoon seasons.

Correlation analyses

The annual variations in dynamic height in the GoT were not consistent with SSH variations. On the other hand, the monsoonal southwest-northeast wind components were consistent with SSH variation. Ekman surface flow was estimated using Equation 1 with the averaged wind stress in the GoT mouth. Fig. 4 shows the interannual variations in SSH, dynamic height in the GoT and inflow/outflow of Ekman volume transport by northeasterly/southwesterly wind stress. Simple and multiple correlations between these three variables were analyzed.

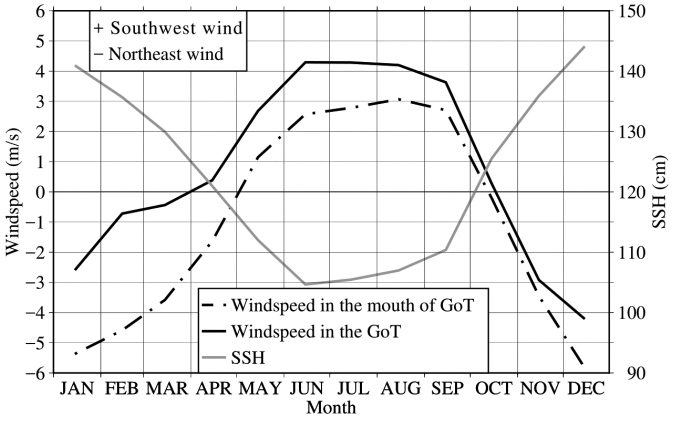

Fig. 3 Averaged annual variation during 7 yrs in sea surface height (SSH) in the Gulf of Thailand (GoT) and averaged wind speed of southwest components within the GoT (area A' in Fig. 1) and at the mouth of the GoT (area B in Fig. 1)

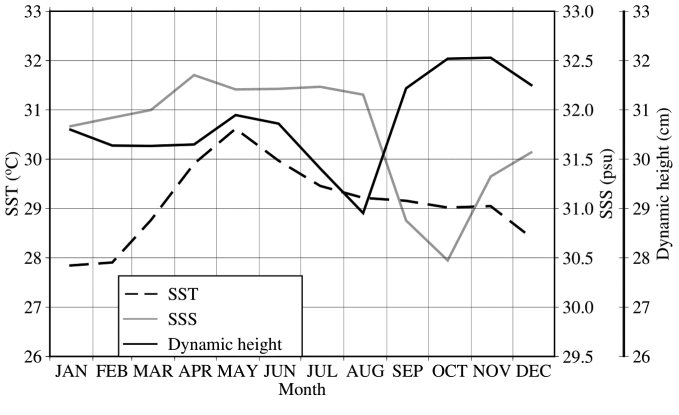

Fig. 2 Averaged annual variations during 7 yrs in sea surface temperature (SST), sea surface salinity (SSS) and dynamic height in the Gulf of Thailand

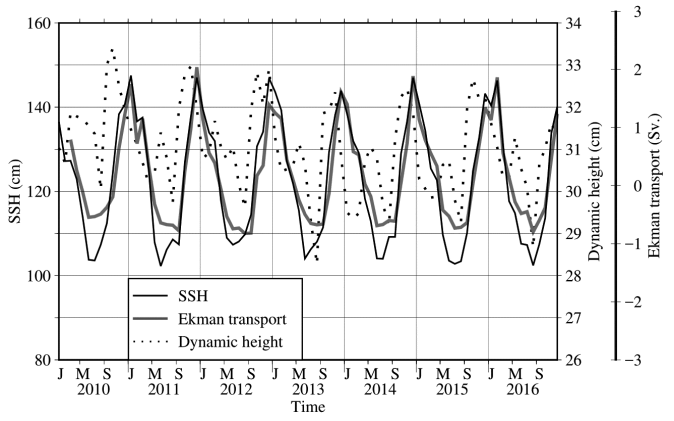

Fig. 4 Interannual variation in sea surface height (SSH) and dynamic height in the Gulf of Thailand (GoT) and estimated Ekman volume transport through the GoT mouth, where J = January, M = May, S = September

Multiple linear regression analyses were carried out (Table 1) for SSH (objective variable), dynamic height and Ekman volume transport (explanatory variables). First, a small, simple correlation coefficient between dynamic height and Ekman volume transport (0.257; $p < 0.2$, n=83) was obtained to avoid multicollinearity. Simple correlation coefficients between SSH and dynamic height, and SSH and Ekman volume transport were 0.368 ($p < 0.01$, n = 83) and 0.955 ($p < 0.01$, n = 83), respectively. The multiple correlation coefficient was 0.964, which was slightly larger than the SSH–Ekman volume transport coefficient. A normalized relational equation of multiple correlations derived from Table 1 is shown in Equation 2:

$$Y = 0.922X_1 + 0.131X_2 \quad (2)$$

where Y is SSH, X_1 is Ekman volume transport and X_2 is dynamic height. For this equation, the Ekman volume transport coefficient (0.922) was approximately seven times larger than that of dynamic height (0.131). This suggested that Ekman transport had a large effect on SSH in the GoT. However, the effect of dynamic height should not be ignored. It can be assumed that the effect would be larger if full-depth fine vertical hydrographic data were to be integrated.

Interannual variation and Water Exchange

It is important to determine which factors control the shifting of the monsoon period or the intensity of the monsoon winds or both. Global climate change is expected to affect monsoon systems (for example, Saji et al., 1999; Tozuka et al., 2011). Therefore, the Indian Ocean Dipole (IOD), which is associated with major oceanic climate change in the Indian Ocean, was analyzed, and the relationship between the IOD and conditions in the GoT was considered in this study. Fig. 5 shows the variations in the Dipole Mode Index (DMI) for January 2010 to December 2016, given by the Japan Agency for Marine-Earth Science and Technology. Pant et al. (2015) reported that when DMI is equal to or greater than +0.5, IOD is extremely positive. Fig. 6 shows two correlation charts, where Fig. 6A shows the correlation between the integrated southwesterly wind speed (x-axis) and deviation of SSH (y-axis) in the GoT, while Fig. 6B shows the correlation between the integrated northeasterly wind speed in the GoT mouth (x-axis) and SSH deviation in the GoT (y-axis). The data for the period of extremely positive IOD were plotted as open circles. In Fig. 6A, open circles gathered at an area where the integrated southwesterly wind speed was high and SSH was lower. In the southwesterly monsoon period, SST in the eastern Indian Ocean (Gulf of Bengal) decreased to lower than normal, and stronger down flow enhanced the high-pressure system in the Gulf of Bengal. Therefore, Fig. 6A suggests that when positive IOD occurred in the southwesterly monsoon period, the horizontal pressure difference between ocean and land could enhance the southwesterly wind, so that SSH in the GoT was reduced due to strong Ekman transport. In Fig. 6B, the influence of IOD was unclear.

Integrated monthly Ekman volume transport was much larger than the estimated water volume change in the GoT between sequence two months from the difference of monthly average SSH and the surface area of GoT (270,000 km^2). If Ekman volume transport could be kept within the GoT, SSH would increase by approximately 16 m during the northeasterly monsoon season (the actual SSH variation within one month was about 10 cm; Fig. 3). Therefore, most of the surface Ekman volume transport was balanced by deep layer flow that was inward deep flow during the southwesterly monsoon season and outward deep flow across the GoT mouth during the northeasterly monsoon season. In fact, temperature distribution maps (not shown) at 50 m depth during the southwesterly monsoon season showed low temperature (<27ºC) water intrusion from the SCS into the GoT along the Malay Peninsula. On the other hand, during the northeasterly monsoon season, warm water (>29ºC) filled 50 m depth in the GoT, with the northwestern side of the GoT being especially warmer. These were consistent with the results of Sojisuporn et al., (2010), which showed the dominant upwelling/downwelling area calculated from surface divergence/convergence flows in the GoT during southwesterly/northeasterly monsoon season, respectively. Buranapratheprat et al. (2016) indicated water intrusion in deep layers of the SCS in southwesterly monsoon season from their local model results. They additionally deduced that Ekman transport by northeasterly monsoon winds maintained the low salinity of GoT surface water. Their results also coincided with the current estimation of seasonal exchange in the water exchange system. In the southwesterly monsoon season, estuarine water exchange developed, while in the northeasterly monsoon season, inverse estuarine water exchange developed. Under such water exchange in relation to the total amount of water volume in the GoT, the replacement rate was 0.53–1.80 yrs during the southwesterly monsoon season and 0.23–1.26 yrs in the northeasterly monsoon season. The most efficient water exchange was recorded in December 2011–January 2012 in the northeasterly monsoon season and in August–September 2012 during the strongest IOD in the southwesterly monsoon season.

Conflict of Interest

The authors declare that there are no conflicts of interest.

Table 1 Basic statistics of correlations

Objective variable	Explanatory variables	Correlation coefficient	Significance level (%)	Number of data (n)
Dynamic height	Ekman transport	0.257	>98.0	83
Sea surface height	Dynamic height	0.368	>99.9	83
Sea surface height	Ekman transport	0.955	>99.9	83
Sea surface height	Ekman transport Dynamic height	0.964	>99.9	83

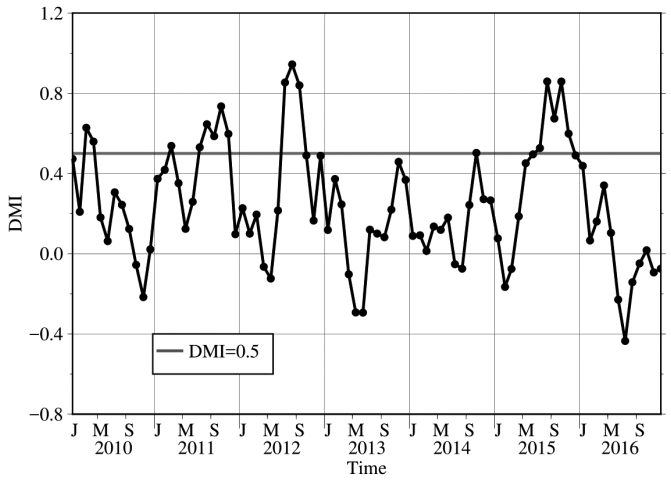

Fig. 5 Time series of monthly Dipole Mode Index (DMI) from 2010 to 2016, where horizontal line shows critical level (DMI = +0.5) of extremely positive Indian Ocean Dipole and J = January, M = May, S = September

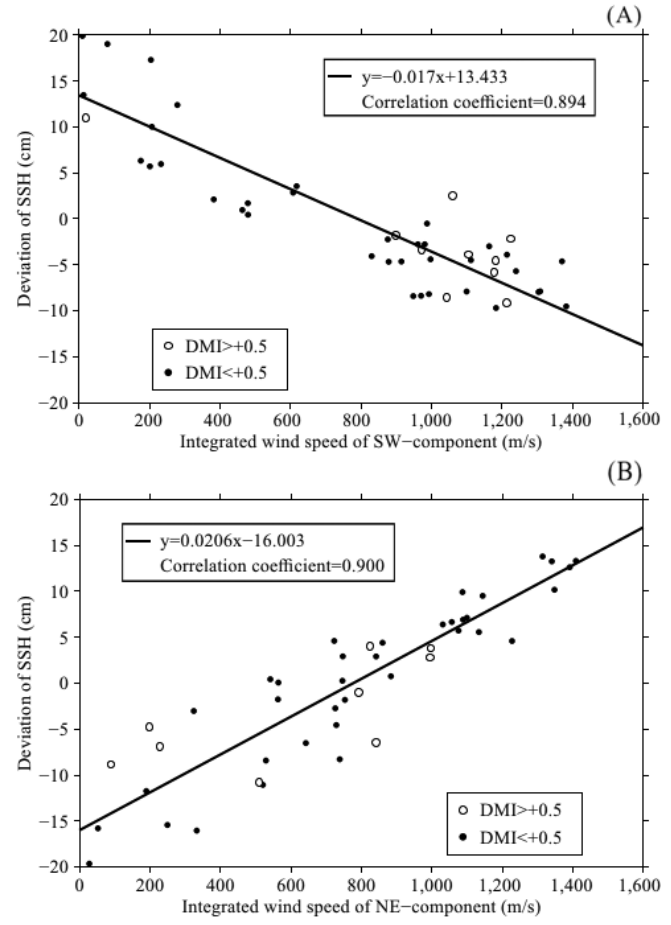

Fig. 6 (A) Correlation of integrated wind speed (X) in the Gulf of Thailand (GoT) and deviation of sea surface height (SSH) in the GoT (Y) during southwesterly monsoon periods; (B) correlation of integrated wind speed in the GoT mouth (X) during northeasterly monsoon periods, where open and filled circles denote data where the Dipole Mode Index (DMI) is over +0.5 and below +0.5, respectively.

Acknowledgements

The authors express their thanks for helpful comments provided by the Journal review process. The authors also thank COPERNICUS for their valuable data service.

References

Bentamy, A. 2017. Quality information document for the Global Ocean Wind Products WIND_GLO_WIND_L4_REP_OBSERVATIONS_012_003. © EU Copernicus Marine Service – Public. http://marine.copernicus.eu/, 2 November 2019.

Buranapratheprat, A., Luadnakrob, P., Yanagi, T., Morimoto, A., Qiao, F. 2016. The modification of water column conditions in the Gulf of Thailand by the influences of the South China Sea and monsoonal winds. Cont. Shelf Res. 118: 100–110. doi.org/10.1016/j.csr.2016.02.016

Cheevaporn, V., Menasveta, P. 2003. Water pollution and habitat degradation in the Gulf of Thailand. Mar. Pollut. Bull. 47: 43–51. doi.org/10.1016/S0025-326X(03)00101-2

Driesenaar, T., Bentamy, A., Hackett, B., Kloe, J. 2016. Quality information document for the Global Ocean Wind Products WIND_GLO_WIND_L3_NRT_OBSERVATIONS_012_002, WIND_GLO_WIND_L4_REP_OBSERVATIONS_012_ 003. © EU Copernicus Marine Service – Public. http://marine.copernicus.eu/, 2 November 2019.

Pant, V., Girishkumar, M.S., Bhaskar, T.V.U., Ravichandran, M., Papa, F., Thangaprakash, V.P. 2015. Observed interannual variability of near-surface salinity in the Bay of Bengal. J. Geophys. Res.: Oceans. 120: 1–15. doi.org/10.1002/2014JC010340

Pauly, D., Chuenpagdee, R. 2003. Development of fisheries in the Gulf of Thailand large marine ecosystem: Analysis of an unplanned experiment In: Hempeland, G., Sherman, K. (Eds.). Large Marine Ecosystems of the World 12: Change and Sustainability. Elsevier Science. Amsterdam, the Netherlands, pp. 337–354.

Pedlosky, J. 1987. Geophysical Fluid Dynamics, 2nd ed. Springer-Verlag. New York, NY, USA.

Qiao, S., Shi, X., Fang, X. et al. 2015. Heavy metal and clay mineral analyses in the sediments of Upper Gulf of Thailand and their implications on sedimentary provenance and dispersion pattern. J. Asian Earth Sci. 114: 488–496. doi.org/10.1016/j.jseaes.2015.04.043

Saji, N.H., Goswami, B.N., Vinayachandran, P.N., Yamagata, T. 1999. A dipole mode in the tropical Indian Ocean., Nature 401, 360–363. doi.org/10.1038/43854

Sojisuporn, P., Morimoto, A., Yanagi, T. 2010. Seasonal variation of sea surface current in the Gulf of Thailand. Coast. Marine Sci. 34: 91–102. doi.org/10.15083/00040677

Tozuka, T., Doi, T., Miyasaka, T., Keenlyside, N., Yamagata, T. 2011. Key factors in simulating the equatorial Atlantic zonal sea surface temperature gradient in a coupled general circulation model. J. Geophys. Res. 116, C06010, doi.org/10.1029/2010JC006717.

Trisirisatayawong, I., Naeije, M., Simons, W., Fenoglio-Marc, L. 2011. Sea level change in the Gulf of Thailand from GPS-corrected tide gauge data and multi-satellite altimetry. Global Planet. Change. 76: 137–151. doi.org/10.1016/j.gloplacha.2010.12.010

Verbrugge, N. 2018a. Product user manual for Global Ocean Multi Observation Products MULTIOBS_GLO_PHY_REP_015_002. © EU Copernicus Marine Service – Public. http://marine.copernicus.eu/, 2 November 2019.

Verbrugge, N. 2018b. Quality information document for Global Ocean Multi Observation Products MULTIOBS_GLO_PHY_REP_015_002. © EU Copernicus Marine Service – Public. http://marine.copernicus.eu/, 2 November 2019. .

Vongvisessomjai, S. 2006. Will sea-level really fall in the Gulf of Thailand? Songklanakarin J. Sci. Technol. 28: 227–248.

Yanagi, T., Akaki, T. 1994. Sea level variation in the eastern Asia. J. Oceanogr. 50: 643–651. doi.org/10.1007/BF02270497

Yanagi, T., Sachoemar, S.I., Takao, T., Fujiwara, S. 2001. Seasonal variation of stratification in the Gulf of Thailand. J. Oceanogr. 57: 461–470. doi.org/10.1023/A:1021237721368